

FR 8203238

# institut de physique nucléaire

LABORATOIRE ASSOCIÉ A L'IN2P3



IPNC-DRE-82-10

NEW EVIDENCE FOR DEEP-LYING HOLE STRENGTH  
IN  $^{118}\text{Sn}$  AND  $^{207}\text{Pb}$  VIA THE ( $^3\text{He},\text{c}$ ) REACTION  
AT 283 MeV

H. Langevin-Joliot, E. Gerlic, J. Guillot,  
M. Sakai<sup>1</sup>, J. Van de Walle,  
Institut de Physique Nucléaire, BP n° 1,  
91406 ORSAY, France

A. Devaux, P. Force, G. Lendaud,  
Laboratoire de Physique Corpusculaire,  
Université de Clermont-Ferrand, France

<sup>1</sup> Permanent address : Institute of Nuclear Study,  
University of Tokyo, Japan.

16 pages  
UNIVERSITÉ PARIS-SUD

NEW EVIDENCE FOR DEEP-LYING HOLE STRENGTH  
IN  $^{115}\text{Sn}$  AND  $^{207}\text{Pb}$  VIA THE ( $^3\text{He},\alpha$ ) REACTION  
AT 283 MeV

H. LANGEVIN-JOLIOT, E. GERLIC, J. GUILLOT,  
M. SAKAI<sup>1</sup>, J. VAN DE WIELE,  
Institut de Physique Nucléaire, B.P. n° 1,  
91406 ORSAY, France

A. DEVAUX, P. FORCE, G. LANDAUD,  
Laboratoire de Physique Corpusculaire,  
Université de Clermont-Ferrand, France

Abstract

It is found that neutron pick-up cross sections up to 50 MeV excitation energy in  $^{115}\text{Sn}$  and  $^{207}\text{Pb}$  may account for the total sum rule strength of all inner shells. The  $^{115}\text{Sn}$  spectrum exhibits much more pronounced structure than that for  $^{207}\text{Pb}$ ; in particular the results give first evidence for a concentration of the  $1f_{7/2}$  strength in a bump centered around 15 MeV. No indication for the predicted strong concentration of the  $1g_{9/2}$  strength in  $^{207}\text{Pb}$  is found.

---

<sup>1</sup> Permanent address : Institute of Nuclear Study,  
University of Tokyo, Japan.

Pick-up reactions have been rather extensively used in the last few years to investigate the deep neutron hole states in medium-weight and heavy nuclei. As a result, the main concentration of the high- $l$  orbital strength belonging to the first inner shell is now well located in a number of nuclei<sup>1-2</sup>). However up to now, results concerning the overall fragmentation, and evidence for deeper-shell contributions to the pick-up residual spectra remain rather scarce<sup>2-9</sup>). One must emphasize that two or three deep sub-shells of different  $l$  values may exhaust a large part of their widely spread strengths in the same region of excitation energy, thus giving complex angular distributions. In this respect, strongly selective reactions and high energy projectiles are desirable.

In this letter, we report on the first results concerning neutron pick-up spectra in heavy nuclei up to an excitation energy of 50 MeV.  $^{116}\text{Sn}$  and  $^{208}\text{Pb}$  targets extensively studied under different conditions were chosen, together with the ( $^3\text{He},\alpha$ ) reaction at the high incident energy of 283 MeV. We have taken advantage of the large mismatching which strongly reduces the smaller  $l$  transfer contributions in each region of excitation energy.

The experiment was performed with the 283 MeV  $^3\text{He}$  beam of the Orsay synchrocyclotron using the achromatic line facility coupled to the spectrometer. The detection system allows the determination of the position and angle of the trajectory at the focal plane and a clean identification of the  $\alpha$  particles. An energy resolution of typically 250 keV was achieved with the targets of enriched isotopes (> 98 %) of thickness 20 mg/cm<sup>2</sup> for  $^{116}\text{Sn}$  and 10 mg/cm<sup>2</sup> for  $^{208}\text{Pb}$ .

Spectra of the ( $^3\text{He},\alpha$ ) reaction on  $^{116}\text{Sn}$  and  $^{208}\text{Pb}$  are displayed in figs. 1a and 1b. The selectivity of this reaction at 283 MeV is demonstrated by the very weak excitation of 2f and 3p valence levels in  $^{207}\text{Pb}$ . It also gives particularly clear evidence for the excitation of the  $1g_{9/2}$  and  $1h_{11/2}$  T > states in  $^{115}\text{Sn}$  and  $^{207}\text{Pb}$  respectively, in spite of their very small spectroscopic factors and their high excitation energies. A main feature of the forward angle spectra is the continuous decrease of the cross-section beyond 20 MeV excitation energy which was not previously observed with lower energy projectiles<sup>4,7-10</sup>.

The  $^{115}\text{Sn}$  spectrum exhibits pronounced structure in the inner hole region above 3.6 MeV. As shown in fig. 1a, the well-known concentration of the  $1g_{9/2}$  strength at 5.3 MeV strongly dominates the spectrum in the present study. In addition, two other bumps are identified. A residual bump appears—subtracting the narrow 5.3 MeV peak—centered at 7.5 MeV with a width of about 5 MeV; the maximum is clearly observed at  $5^\circ$  and  $8^\circ$  (see fig. 1a). A second bump (F) is centered around 15 MeV with a width of the order of 7 MeV. The  $^{207}\text{Pb}$  spectrum at  $2^\circ$  (fig. 1b) presents no such gross structure in addition to the complex bump (A) attributed to the concentration of the  $1h_{11/2}$  strength around 8.3 MeV<sup>8-9</sup>. However, the large angle spectra indicate two smooth bumps with their maxima around 12 and 23 MeV, respectively.

Angular distributions are presented in fig. 2. Following the usual procedure<sup>6-10</sup>, the background subtracted in the inner-hole region was evaluated at the highest excitation energies where the pick-up contribution is most probably very small; this condition is particularly well fulfilled in the present case. The experimental

results are compared with DWBA predictions performed with the program DWUCK 4. The optical model parameters are those of ref<sup>11)</sup> for the entrance channel, with a real depth energy dependence correction, and of ref<sup>12)</sup> for the outgoing channel. Exact finite range calculations performed for some typical cases using the code Mary give only small relative corrections to the Zero-range approximation.

The angular distributions agree rather well with those expected for direct pick-up, with the exception of that of the weak 4.2 MeV group and of the 3.4 MeV level, which is not well separated from adjacent collective states in <sup>207</sup>Pb ; the too small slope observed in those cases is characteristic of important indirect pick-up contributions<sup>3,12)</sup>.

All inner neutron states down to 1s may be expected below 50 MeV. Their contributions have been evaluated for full subshells located at the Hartree Fock energies<sup>13)</sup>. We point out that at this high incident energy, DWBA cross sections at forward angles do not depend much on the separation energy within 15 MeV. The whole experimental cross section for this inner hole region in both nuclei exceeds the prediction for the total sum rule by typically 27 %. In view of all uncertainties this may be considered as a reasonable agreement. The main contributing states in the different energy regions and their relative cross sections are indicated by arrows in fig. 1. One observes that the deepest state contributions are much too small to explain the results beyond 20 MeV. We would thus conclude that a significant part of the larger  $\ell$  hole strengths is spread toward the very high excitation energies ; also the spectrum shape may suggest another mechanism such as pick-up on clusters.

It is interesting to compare the present results concerning the first inner shells with previous results and theoretical predictions. The  $1g_{9/2}$  strength fragmentation in  $^{115}\text{Sn}$  is presented in table 1. Our spectroscopic factors agree rather well with ref<sup>7,10)</sup> and with the predictions of Soloviev et al.<sup>14)</sup> which explain the second maximum here observed at 7.5 MeV. The cross section up to 8.6 MeV may account for nearly all the  $1g_{9/2}$   $T <$  strength.

The experimental angular distribution around 10 MeV (bin E) is best reproduced with  $1g_{9/2}$  and  $1f_{5/2}$  contributions. Siemssen et al.<sup>7)</sup> have first observed a shoulder extending up to 18 MeV in their (d,t) spectra ; they attribute to the  $1f_{5/2}$  hole the corresponding wide bump centered at 10.6 MeV. The ( $^3\text{He},\alpha$ ) spectra exhibit a pronounced bump centered at 15 MeV. The total  $1f_{5/2}$  strength if concentrated either in bin E or in bin F could only explain about 75 % and 35 % of the corresponding cross sections. This, and the good agreement of the angular distribution, lead us to attribute the main contribution to the bump F between 11.5 and 18 MeV to the  $1f_{7/2}$  strength. The matching conditions of the high energy ( $^3\text{He},\alpha$ ) reaction compared to (d,t) at 50 MeV favour the highly excited states around 15 MeV. Our results on the  $1f$  states are summarized in table 2.

In  $^{207}\text{Pb}$ , we find 53 % of the  $1h_{11/2}$  strength in the bump A between 6.6 and 9.8 MeV. One also notices that the experimental cross sections up to 20 MeV (bins A + B) may account for the missing  $1h_{11/2}$  and total  $1g_{7/2}$  and  $1g_{9/2}$  strengths, which was not the case in the previous experiments<sup>8-9)</sup>.

A schematic normalized experimental spectrum is compared in fig. 3 with theoretical predictions for the fragmentation of the  $1h_{11/2}$  hole state<sup>15-16)</sup> and the  $1g_{9/2}$  and  $1g_{7/2}$  states<sup>15)</sup>. The energy scale of ref<sup>15)</sup> and 16) have been shifted down by 2. and 1.2 MeV respectively, which is a compromise, the first  $13/2^+$  and  $9/2^-$  levels coming then too low by 0.5 MeV. Also the bars representative of the  $1g$  fragments have been corrected for the ratio of  $1g$  over  $1h$  pick-up cross sections.

The total  $1h_{11/2}$  strength of the three main fragments of ref<sup>15)</sup> and the corresponding part of the two peaks of ref<sup>16)</sup> are comparable to the experimental result for the bump at 8 MeV. But no strong concentration of the  $1g_{9/2}$  strength could be identified. The experimental spectrum is much smoother than expected and additional spreading has clearly to be introduced. The coupling of the hole state with the  $1$  hole- $2$  phonons states, in addition to the coupling with  $1$  hole- $1$  phonon states, have been shown to play a significant role in the case of tin isotopes<sup>14)</sup>. It would be interesting to evaluate such effects on the spreading of  $1h_{11/2}$  and  $1g$  inner holes in  $^{207}\text{Pb}$ .

In summary, we have demonstrated that the strengths measured with the ( $^3\text{He},\alpha$ ) reaction up to 50 MeV excitation energy may account for the sum-rule of all the neutrons of the inner shells or somewhat more. The  $1g_{9/2}$  hole strength in  $^{115}\text{Sn}$  was clearly observed beyond the strong 5.3 MeV peak, up to about 11.5 MeV. We have also found first evidence for the deep hole  $1f_{7/2}$  strength as a bump centered around 15 MeV. Further experiments are needed to improve our knowledge on deep hole states in heavy nuclei, as well as further theoretical efforts to explain their observed strong fragmentation, especially toward higher excitation energies.

#### REFERENCES

- 1) - M. Sakai and K. Kubo, Nucl. Phys. A185 (1972) 217.
- 2) - G.M. Crawley, Proc. Int. Symp. on highly excited states, Osaka, Japan (1980) ; S. Galès, Nucl. Phys. A354 (1981) 193 and references therein.
- 3) - J. Van de Wiele, E. Gerlic, H. Langevin-Joliot and G. Duhamel, Nucl. Phys. A297 (1978) 61 and references, therein.
- 4) - M. Tamaka et al., Phys. Lett. 78B (1978) 221.
- 5) - T. Ishimatsu et al., Nucl. Phys. A336 (1980) 205.
- 6) - G. Duhamel et al., J. of Phys. G7 (1981) 1415.
- 7) - R.H. Siemssen et al., Phys. Lett. 103B (1981) 323.
- 8) - S. Galès, G.M. Crawley, D. Weber and B. Zwieglinski, Phys. Rev. C13 (1978) 2475.
- 9) - J. Guillot et al., Phys. Rev. C21 (1980) 879.
- 10) - E. Gerlic et al., Phys. Rev. C21 (1980) 124.
- 11) - N. Willis et al., Nucl. Phys. A204 (1973) 454.
- 12) - J. Van de Wiele, Thesis and IPNO Report to be published.
- 13) - M. Beiner, H. Flocard, Nguyen Van Giai and P. Quentin, Nucl. Phys. A238 (1975) 29 and private communication.
- 14) - V.G. Soloviev, C. Stoyanov and A. Vdovin, Nucl. Phys. A342 (1980) 261.
- 15) - V. Bernard and N.V. Giai, Nucl. Phys. A348 (1980) 75.
- 16) - P.F. Bortignon and R.A. Broglia, Nucl. A371 (1981) 405.



## FIGURE CAPTIONS

- Fig. 1a - 1b      Alpha spectra of the  $^{116}\text{Sn} (^3\text{He},\alpha)$  and  $^{207}\text{Pb} (^3\text{He},\alpha)$  reactions recorded at two angles. Some of the energy bins have been chosen for comparison with other results. The position of some subshells as given by Hartree Fock calculations<sup>13)</sup> are indicated by dashed arrows with lengths proportional to the expected cross sections.
- Fig. 2            Angular distributions of valence levels and of inner hole structures decomposed into energy bins as indicated on Fig. 1. The curves are DWBA calculations. Background distributions are given in the insets.
- Fig. 3            Comparison of a normalized schematic experimental spectrum of  $^{207}\text{Pb}$  with theoretical predictions. The solid bars<sup>15)</sup> and solid curve<sup>16)</sup> correspond to  $1h_{11/2}$ ; the dotted and the dashed lines correspond to  $1g_{7/2}$  and  $1g_{9/2}$  (Ref. 15); the reduction factors indicate the ratio of  $1g$  over  $1h_{11/2}$  DWBA cross sections at  $2^\circ$ .

Table 1

Fragmentation of the  $1g_{9/2}$  neutron hole strength in  $^{115}\text{Sn}$ .

$E_x$ (MeV)	BIN Fig. 1a	$c^2s_{\text{exp}}$			$c^2s_{\text{th}}$	
		present work	others		Ref. (14)	
4.8 - 5.8	B	2.9	2.5 <sup>b)</sup>	2.15 <sup>c)</sup>	1.3 <sup>d)</sup>	2.7
3.6 - 6.6	A + B + C	5.6	4.3 <sup>b)</sup>	- 5.7 <sup>c)</sup>	- 2.9 <sup>d)</sup>	4.8
6.6 - 8.6	D	2.4	$\left\{ \begin{array}{l} 5.5c) \\ - 1.6d) \end{array} \right.$		2.6	
8.6 - 11.6	E	1.4 - (2.5 <sup>a)</sup>			-	

- a) without any  $1f_{5/2}$  contribution in BIN E (see table 2)
- b) Ref. (10)
- c) from Ref. (7)
- d) from Ref. (4)

Table 2

$1f_{5/2}$  and  $1f_{7/2}$  neutron hole strengths in  $^{115}\text{Sn}$

$E_x$ (MeV)	BIN Fig. 1a	$\text{C}^{25}\text{S}$		
		Ref. 7 $1f_{5/2}$	this work $1f_{5/2}$	this work $1f_{7/2}$
8.6-11.6	E	} 8.6	3.5-(8 <sup>a</sup> )	-
11.6-18.5	F		2.1-(17 <sup>a</sup> )	9.4

a) without contributions of  $1g_{9/2}$  in bin E (see table 1) and  $1f_{7/2}$  in bin F.

Fig. 1a - 1b

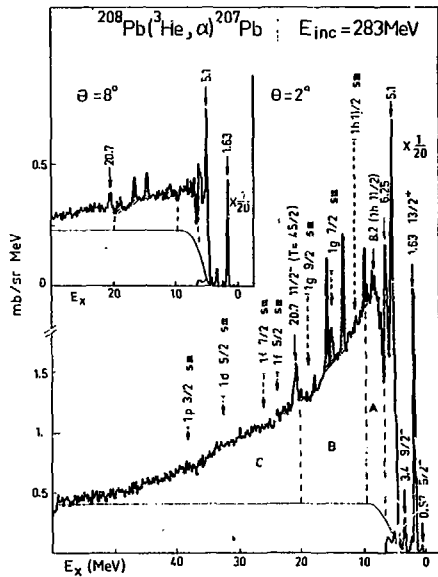
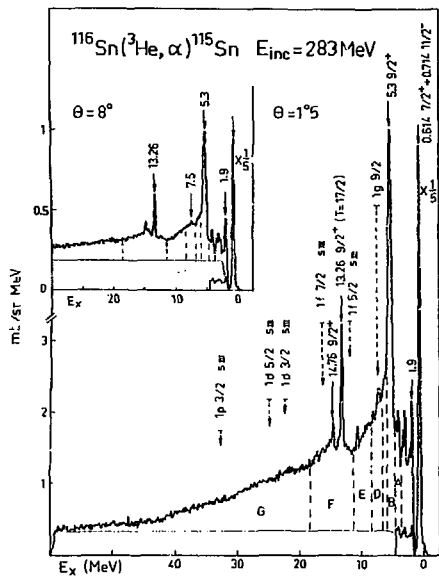


Fig. 2

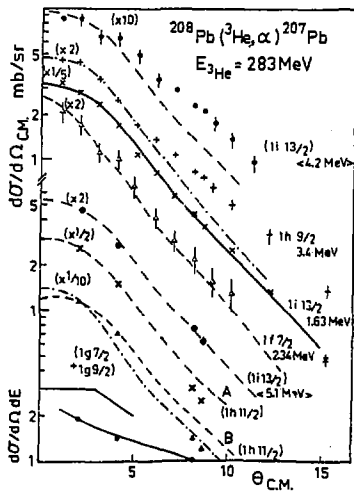
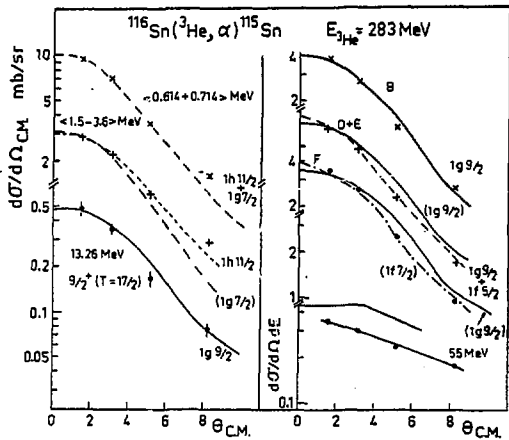


Fig. 3

